ANNALI DI GEOFISICA, VOL. XXXIX, N. 1, January 1996

# Some considerations on the use of the geoelectric «square» array

**Fulvio Merlanti and Mauro Pavan**
*Dipartimento di Scienze della Terra, Università di Genova, Italy*

**Abstract**
The «square array» is what we may consider to be an unconventional geoelectric configuration since it is not widely used and therefore there are few examples of practical application. The purpose of this research was to verify the operating effectiveness of this configuration in terms of profile and sounding, and the significance of the set of possible measurements and derived parameters. This was also obtained by comparing the relative measurements with the most common linear arrays (Wenner, Schlumberger, tripotential). The experiment was carried out in two different zones. In the first area, corresponding to the archaeological site of Marzabotto (Bologna), the target was represented by wall remnants inserted in a substantially homogeneous medium, from an electrical point of view, and at depths that are less than those of the dimensions of the device used. At the second site, located in the valley of Landrazza (Savona), the situation was very different, with a valley section on a calcareous bedrock filled with poorly classified residual sediments. An overall analysis of the results showed that the square technique is more exhaustive than the classical linear arrangements when performing soundings. Instead, with regard to profile development, it is not as preferred since it involves a greater amount of work without generating improved information. From analysis of the experimental results, considerable doubts arose about the meaning and the use of the anisotropy coefficients and the error term as defined theoretically. These parameters turned out to be of little use with regard to the characterization of the ground anisotropy and for checking the reliability of the measurements.

**Key words** *applied geophysics – electrical prospecting – square array*

## 1. Introduction

A standard geoelectric configuration with four electrodes may take the shape of any irregular quadrilateral. In general, a regular linear configuration is preferred because it is much simpler to represent and process the relative data. When a linear array with equally spaced electrodes is considered, there are three possible basic configurations (fig. 1a): $\alpha$, $\beta$ and $\gamma$. In considering also a homogeneous ground, the general linearity of response implies that, like reciprocity, the principle of superposition will also hold. Assuming, finally that $V_M > V_N$, we can provide for the three different resistance measurements: $R_\alpha$, $R_\beta$ and $R_\gamma$, the relations reported by Habberjam (1979, p. 20):

$$\begin{aligned} R_\alpha &= \Phi_{12} + \Phi_{34} - \Phi_{13} - \Phi_{24} \\ R_\beta &= \Phi_{14} + \Phi_{23} - \Phi_{24} - \Phi_{13} \\ R_\gamma &= \Phi_{12} + \Phi_{34} - \Phi_{23} - \Phi_{14} \end{aligned} \qquad (1.1)$$

From (1.1) we can easily obtain the relation:

$$R_\alpha = R_\beta + R_\gamma \qquad (1.2)$$

A formula like (1.2) can be obtained for each particular array, and it is normally indicated as the Tripotential Condition (Carpenter, 1955; Carpenter and Habberjam, 1956). In general, when tripotential measurements are

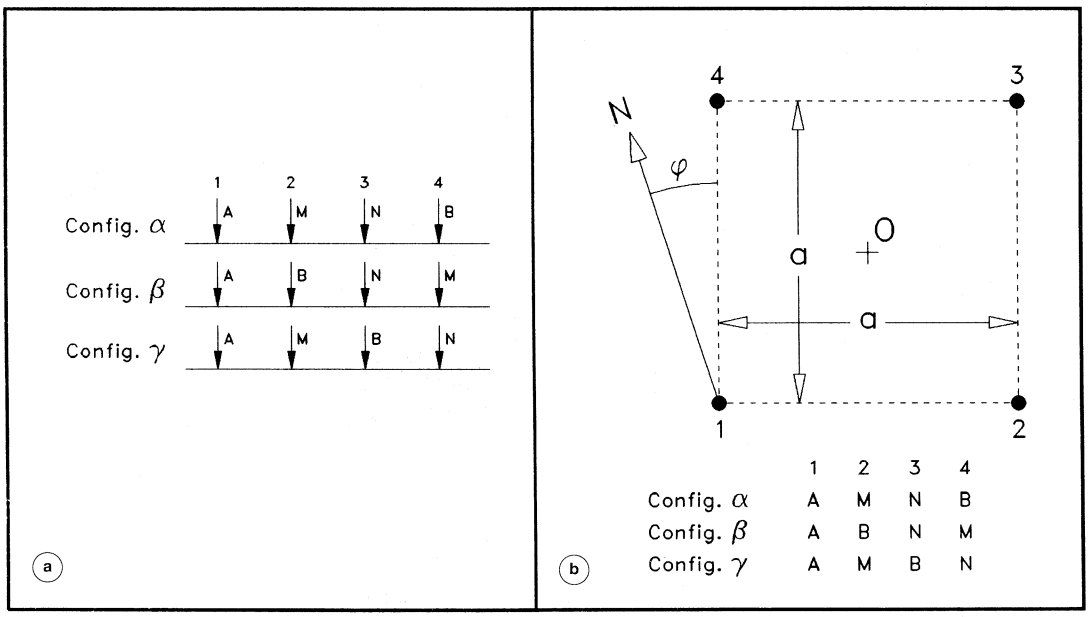


**Fig. 1a,b.** Different configurations which can be obtained with: a) a generic linear quadripolar array; b) a square array.

performed, there is a small discrepancy in the tripotential condition, so that:

$$R_\alpha - R_\beta - R_\gamma = \varepsilon \tag{1.3}$$

or one can introduce a relationship:

$$v = \frac{\varepsilon}{|R_\alpha| + |R_\beta| + |R_\gamma|} \tag{1.4}$$

where the ratio (1.4) is called the Tripotential Error. The relations (1.3) or (1.4) can be used to control the goodness of measurements.

The square array represents a particular configuration of the generic array with four electrodes. In this arrangement the electrodes are positioned at the vertices of a square. The configurations with this array, as reported in fig. 1b, are very similar to those previously indicated. The square has a length $a$ and a center at O $(x, y)$. In addition, $\varphi$ is used to indicate the direction of the array, assuming that $\varphi$ is the angle formed from side 14 (fig. 1b) with the North. However, the square array samples resistance values $R_\alpha$, $R_\beta$, and $R_\gamma$ in different directions. Each value is attributed to the position of the center O with respect to the adopted reference system. In homogeneous soil, $R_\alpha$ is equal to $R_\beta$, and $R_\gamma$ will be zero. The values of apparent resistivity $\rho_\alpha$ and $\rho_\beta$ are significant of the behavior of the apparent resistivity in two different and mutually perpendicular directions, corresponding to the configurations $\alpha$ and $\beta$, respectively of:

$$\rho_\alpha = \frac{2\pi a R_\alpha}{2-\sqrt{2}} \quad \text{and} \quad \rho_\beta = \frac{2\pi a R_\beta}{2-\sqrt{2}}. \tag{1.5}$$

These two measurements can be combined to create a mean resistivity:

$$\rho_m = \frac{\rho_\alpha + \rho_\beta}{2}. \tag{1.6}$$

To accentuate any directional effects starting from the resistivity measurements, parameters can be introduced and identified under the general name of anisotropy coefficients. In an

anisotropic half space, the apparent resistivity is not only a function of the coordinates of the electrodes $(x, y)$ and their relative distance $r$, but it will also be a function of the orientation angle $\varphi$ of the array:

$$\rho = f(x, y, r, \varphi). \tag{1.7}$$

As a consequence, the apparent resistivity becomes a function of four parameters, which when completely analyzed provide a description of the lateral variations. For the sake of simplicity, if we consider two equal arrays $a$ and $b$ with two electrodes (mutually perpendicular), we obtain two resistivity measurements that can be combined to produce an average resistivity:

$$\rho_m(\varphi) = \frac{\rho_a + \rho_b}{2} \tag{1.8}$$

where $\varphi$ is the orientation of the device. With the same resistivity values, we can obtain the definition of the Azimuthal Inhomogeneity Ratio (AIR) as:

$$\mathrm{AIR}(x, y, r, \varphi) = \frac{(\rho_a - \rho_b)}{\rho_m(x, y, r, \varphi)} =$$

$$= 2\,\frac{\rho_a - \rho_b}{\rho_a + \rho_b} = 2\,\frac{R_a - R_b}{R_a + R_b}. \tag{1.9}$$

The average resistivity and the AIR were defined for an array with two electrodes which, in practice, has very limited use. However, there are no limitations because these relationships are extended to any configuration with 3 or 4 electrodes and, in particular, to a symmetrical situation such as the one provided by the square array. The AIR can be calculated in two different ways:

$$\mathrm{AIR}(\alpha - \beta) = 2\,\frac{\rho_\alpha - \rho_\beta}{\rho_\alpha + \rho_\beta} = 2\,\frac{R_\alpha - R_\beta}{R_\alpha + R_\beta} \tag{1.10}$$

$$\mathrm{AIR}(\gamma) = 2\,\frac{R_\gamma}{R_\alpha + R_\beta}. \tag{1.11}$$

In (1.10), the numerator is the difference between the resistances $R_\alpha$ and $R_\beta$ indicated afterwards as $\mathrm{AIR}(\alpha-\beta)$. The $\mathrm{AIR}(\alpha-\beta)$ can be expressed as a function of $\rho$ or $R$ because the geometrical factors are the same for both configurations. Instead, (1.11) is based on the tripotential condition, setting the numerator to the value of $R_\gamma$, which is indicated afterwards as $\mathrm{AIR}(\gamma)$. $\mathrm{AIR}(\alpha-\beta)$ can be usefully applied to profiles because of its directionality. The parameter $\mathrm{AIR}(\gamma)$ generally has a more regular development than $\mathrm{AIR}(\alpha-\beta)$.

Considering only resistivity soundings, other anisotropy coefficients may be defined. In fact, it is known that the lateral variations of resistivity are the main source of uncertainty in the interpretation of the soundings. To compensate for this problem, we can use special configurations such as the Offset Wenner (Barker, 1981) in which by analyzing tripotential measurements it is possible to characterize the deviation from the theoretical condition of horizontal stratification.

The square array provides a similar but more compact operational configuration. In this system, expansion occurs with the increase of the sides of the square by a factor of $\sqrt{2}$ while fixing the center and the orientation of the array. The configurations $\alpha$, $\beta$ and $\gamma$ are selected, similarly to the Offset Wenner array, directly by the control devices of a multielectrode line (Merlanti, 1990). Again, in this case, the tripotential condition helps to control the measurements.

Starting from the measurements $\alpha$ and $\beta$, for each spacing, we obtain an average resistivity value and a corresponding AIR value. The set of measurements produces a resistivity curve related to the particular orientation of the array. The AIR value is highly influenced by this orientation and if the array is positioned at 45° from the electric strike, that strike is not observable.

From the AIR values, it is also possible to define, for each single spacing of the array, an Azimuthal Inhomogeneity Index (AII), as the root mean square of the AIR. Even this coefficient is closely related to the orientation of the device and may be zero in particular conditions of lateral resistivity distribution.

The anisotropy coefficients introduced involve a simple square array, which by sam-

pling two perpendicular directions for each spacing, provides a stable measurement of the apparent resistivity with respect to the orientation. At the same time, it also provides a control, through the AIR, of the existence or non-existence of directional effects. However, it was observed that in stratified mediums with major inclinations or that are particularly anisotropic, very wide orientational effects may be encountered which alter the stability of the resistivity values. Under these conditions, it is preferred to introduce, as proposed by Habberjam (1972), a variation to the square array: the crossed square array. This is a combination of the classical square array and another square array, with a center that coincides with the first one and with diagonals rotated at 45° with respect to the former.

Even the crossed square array provides three resistances $R'_\alpha$, $R'_\beta$ and $R'_\gamma$ to which it is possible to apply the tripotential condition. In this configuration two average resistivities may be derived, $\rho_m$ and $\rho'_m$, one for each orientation, and therefore a main average resistivity $\rho_M$. From the six resistivity measurements performed with the normal and crossed square array, the two $\gamma$ measurements may be used as a control and to correct any small differences.

## 2. Experimental results of the square array measurements

The previous section provided a brief summary of the theoretical characteristics of the parameters that can be derived from the measurements performed with a square array. Now let us examine the real effectiveness of such an approach under experimental conditions. It should be mentioned that the utility of the square array, whether the simple or crossed version, does not only involve resistivity soundings. In fact, its application may be extended to profiling operations, *i.e.* conditions in which the lateral variations in resistivity must be solved at what are rather surface ground levels. By combining various profiles, obtained with constant spacing and fixed array dimensions, it is possible to obtain an areal representation of the parameters measured (or derived) by means of maps. However, it should be recalled that the measurement obtained with a square array is normally assigned to the coordinates of the center of active square. Therefore, it follows that the representations by profiles and by maps may provide rather different developments within the anomaly representation.

The experimental examples which follow refer to two completely different environments; however, they are quite representative of real and widespread situations. The dimensions

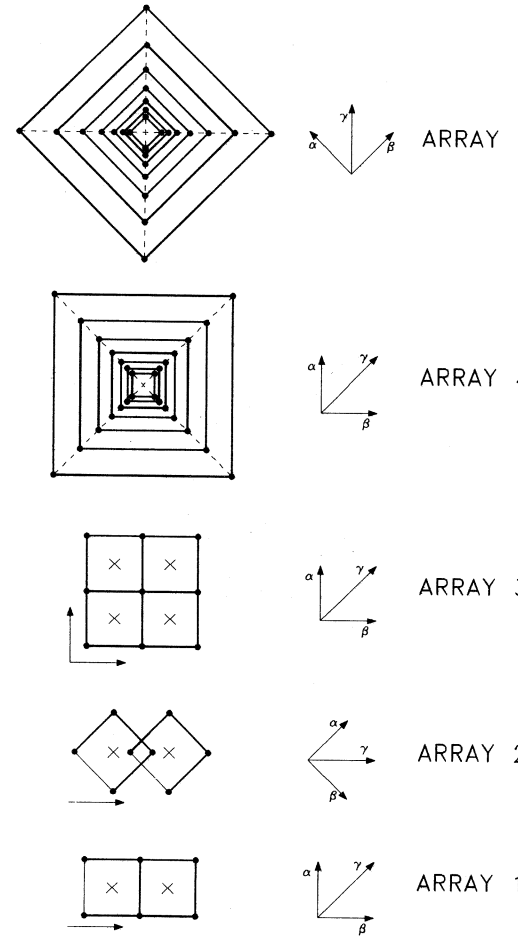


**Fig. 2.** Various configurations able to perform profiles, maps and soundings with the square array.

classify the experiments within the shallow geophysics but, considering the scale factors involved, the conclusions may be considered to have general validity.

Figure 2 reports the various application schemes of the square array which are used in prospecting to which reference will be made in the following description of the results. The positions of the electrodes and the «directions» of the various types of resistivity are indicated for each configuration.

## 3. Square measurements in the archaeological site of Marzabotto

The archaeological site of Marzabotto (Bo) is located to the south of the actual town and rises on a terrace surrounded by a meander of the Reno river. The site includes the remains of a vast anthropic area corresponding to an ancient Etruscan settlement that dates back to the VI and V centuries B.C. (Sassatelli, 1989). The site is divided into regions, which are then broken down into insulae. Integrated geophysical measurements were performed in one of these insulae (Bozzo *et al.*, 1994).

Figure 3 illustrates the map of the survey area (corresponding to insula 2 of region IV) with the anomalous bodies obtained supplied by the classical tripotential measurements and verified with shovel tests (Sassatelli and Brizzolara, 1990). The shovels performed to verify this information have shown that these anomalies correspond to the remains of foundations located at a depth of about 0.5 m and consist of sandy pebbles with various dimensions. The interruptions are caused by diggings relative to agricultural activities which have damaged many of the wall structures to a considerable depth. Other developments, such as the one shown in profile 9, characterized by the matching results of $\rho_\alpha$ and $\rho_\beta$, were found to correspond with the remains of an artesian well. The bodies extend mainly in the N-S direction and, secondarily, in the E-W direction. This last direction was selected to develop the profiles with a square array since it is the best direction for measuring maximum and minimum resistivities $\rho_\alpha$ and $\rho_\beta$. In addition, it was decided to

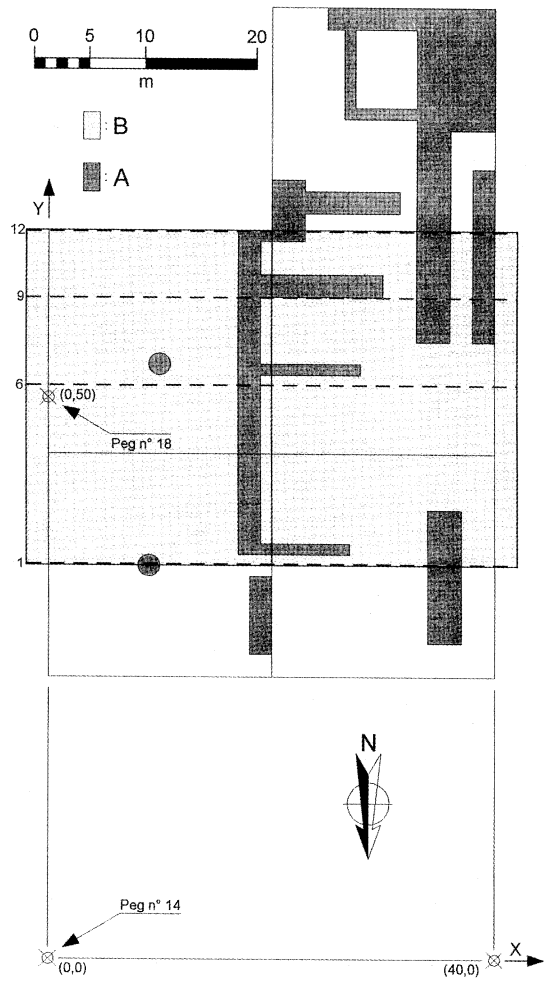


**Fig. 3.** Marzabotto. B) area surveyed with a square array; A) main elements detected with other geophysical techniques and verified with shovel tests.

use a side dimension of 2 m in relation to the dimensions of the buried structures and their assumed interment depth.

Figure 4 reports several profiles performed with configuration 1 shown in fig. 2. It can immediately be seen how, in several parts, high resistivity values of $\rho_\alpha$ correspond to minimum values of $\rho_\beta$ and *vice versa*. The fact that this behavior does not extend throughout the profile means that there are alternating strips of

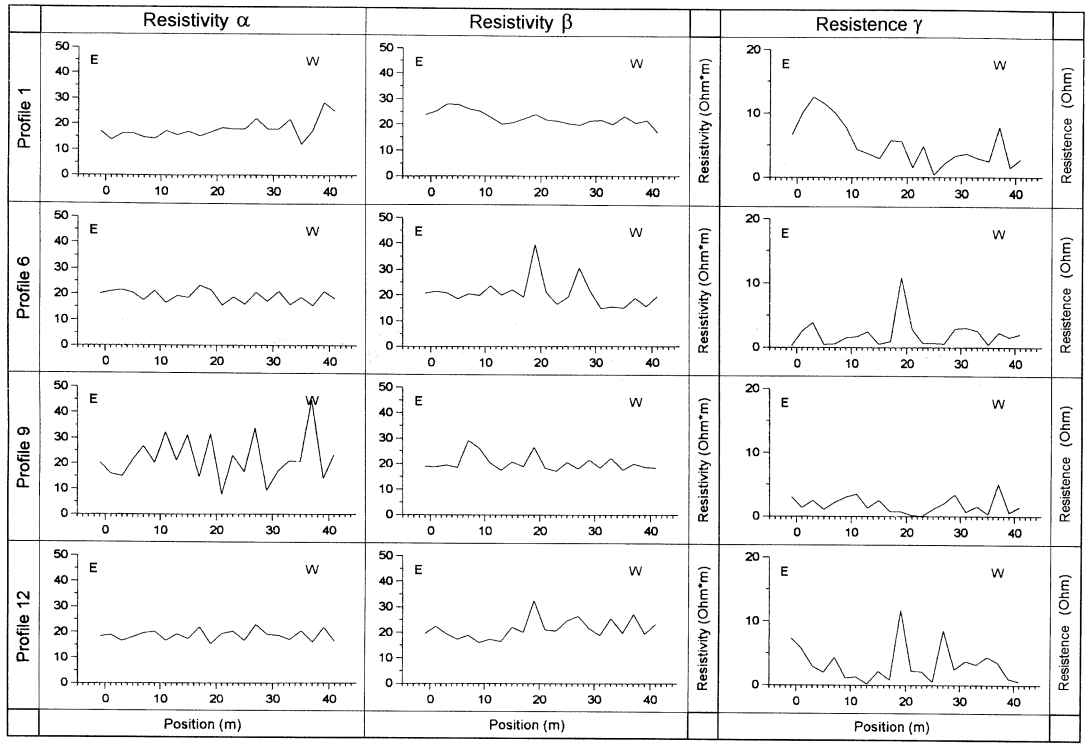


**Fig. 4.** Marzabotto. Examples of some square profiles. Parameters $\rho_\alpha$, $\rho_\beta$ and $R_\gamma$.

homogeneous ground and anisotropic sectors which are particularly enhanced by the directional effect of the square array.

Comparing the developments of $R_\gamma$ with those of the corresponding $\rho_\alpha$ and $\rho_\beta$ values, it can be seen that, generally, the areas with a greater $R_\gamma$ correspond to the areas in which $\rho_\alpha$ and $\rho_\beta$ have the opposite developments. Instead, the same profiles $R_\gamma$ do not exhibit any maximum corresponding to the well where $\rho_\alpha$ and $\rho_\beta$ have correlated behavior. It is probable that to increase the physical meaning of $R_\gamma$ it is necessary to acquire the two possible values with the square configuration, and not only one as indicated by operating practices.

In all profiles (fig. 5) the AIR$(\alpha-\beta)$ development tends to exhibit rapid oscillations. This is characteristic of all the tripotential configurations (and therefore like square) where there is a counterphase development corresponding to the structures whose dimensions are comparable to those of the device. Error $v$ development is always represented in fig. 5 together with that of AIR$(\gamma)$. It assumes very high values compared to the prospected theoretical values (about 1%). In practice, we find that this type of limit cannot have any practical meaning considering the electric and geometric approximations involved in calculating the derived parameters (resistance, resistivity and AIR). Realistically, the definition of the acceptable limit of error $v$ must include a corrective factor of at least 10 (therefore increasing to values of about 10%).

However, there is another consideration that leads to doubts about the use of this type of parameters. In fact, observing the developments of the AIR$(\alpha-\beta)$ values, we find that such

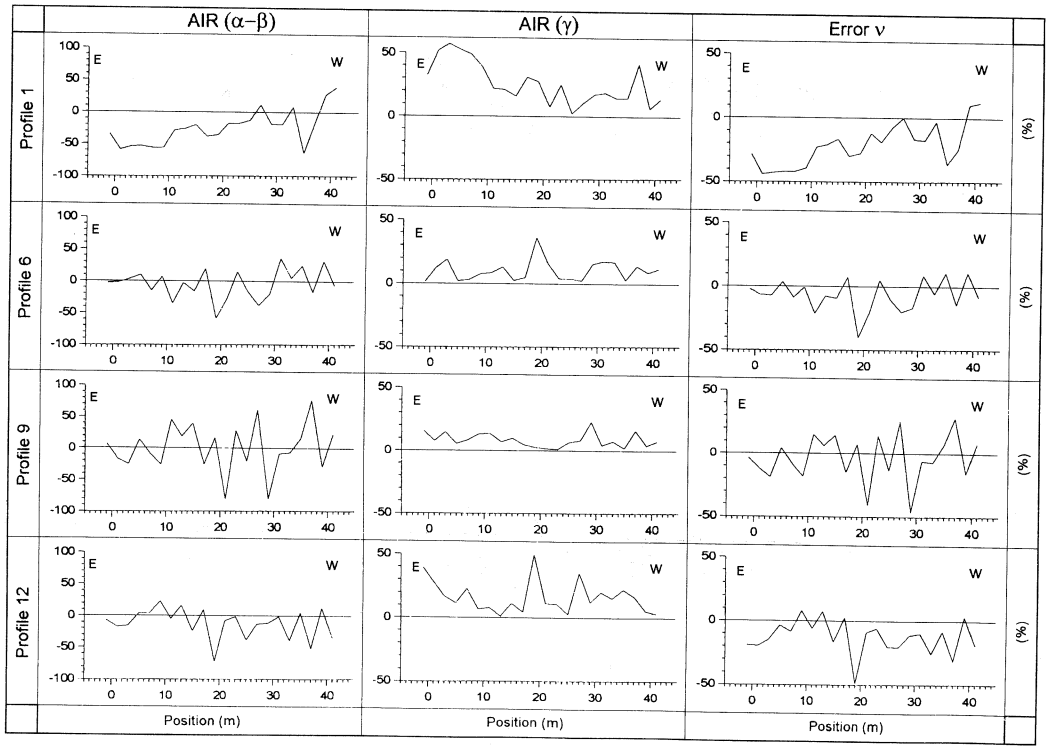


**Fig. 5.** Marzabotto. Parameters: AIR$(\alpha-\beta)$, AIR$(\gamma)$ and error term $v$ for the same profiles shown in fig. 4.

values behave, profile by profile, in a way that is completely similar to that of the error term $v$. This indicates that the error $v$ being derived analytically from the definition of the AIR$(\alpha-\beta)$, it makes no supplemental knowledge contribution to the analysis of the square measurements on the profiles.

The bidimensional correlation among all the profiles is reported in fig. 6a-c in the form of resistivity maps obtained with configuration 3 of fig. 2. The map relative to resistivity $\rho_\alpha$ (fig. 6a) indicates: the positive anomaly (A) connected to a wall structure that extends continuously in the N-S direction; the anomalies (B) and (C) are also connected to wall structures but they are locally interrupted or lowered; anomaly (D) which, despite its apparent E-W development, is correlated with a well entrance centered on the coordinates (8,52).

The map of the resistivities $\rho_\beta$ (fig. 6b) clearly reproduces some of the structures mentioned (A and C) but others are not so clear, (B) for example. An anomaly, (E), which develops along the E-W direction, is evident only in this map. Anomaly (D) is clear and more defined. The map relative to the average resistivity $\rho_m$ (fig. 6c) shows how this parameter tends to normalize the situation offering a more regular identification of sectors involved with structural remains.

It should be emphasized how the transverse dimensions of the anomalies are two to four times greater than the real dimensions of the buried structures, as shown by the shovel tests. Therefore, it can be stated that the square array is sensitive to the lateral conditions also when the sources of the anomaly are not completely included to the interior of the electrode square.

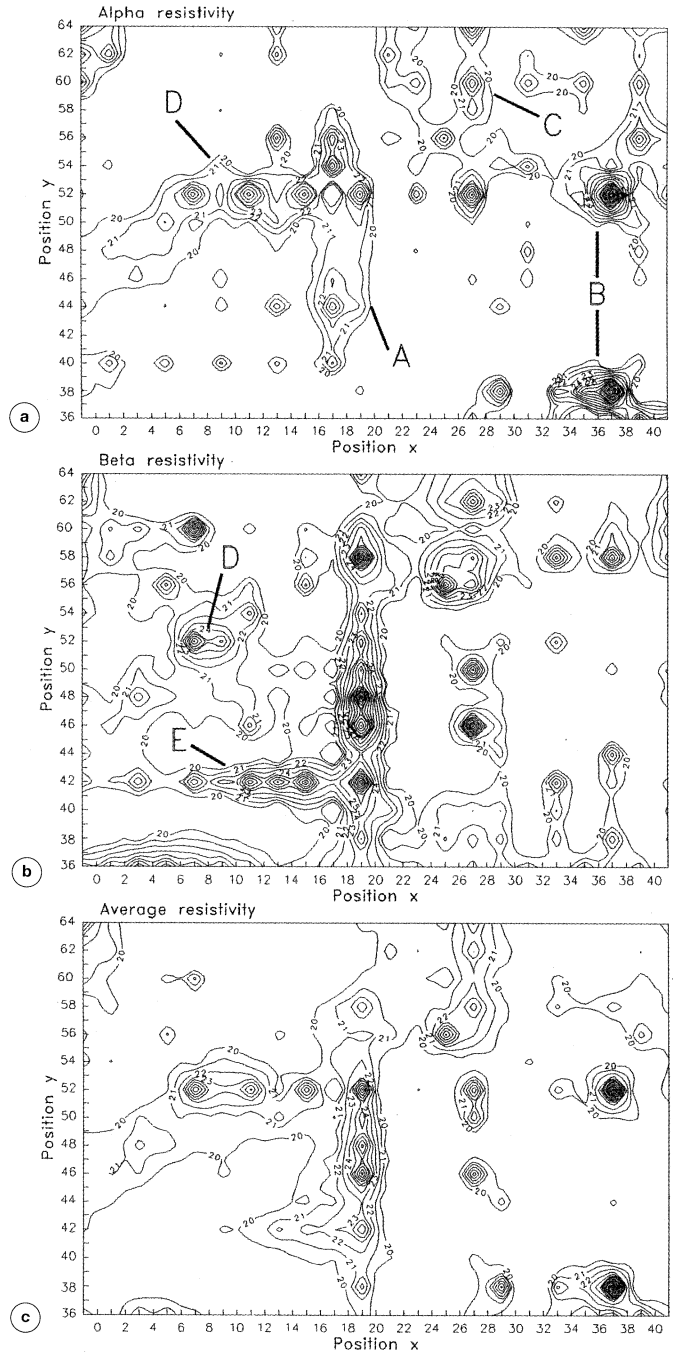


**Fig. 6a-c.** Marzabotto. Maps of the areal correlations of the square measurements in area (B) of fig. 3. a) Resistivity $\rho_\alpha$; b) resistivity $\rho_\beta$; c) average resistivity $\rho_m$. Resistivity values in Ohm.m.

The AIR($\alpha-\beta$) and AIR($\gamma$) coefficients were not suitable for a simple bidimensional representation since they exhibit typically «spotted» forms where the high frequency dominates all the other components. In this case, filtering is needed to remove the useful components to represent the buried structures. But considering what was mentioned about the significance of these parameters, efforts in this way do not seem to be justified.

## 4. Square measurements in the Landrazza valley (Sv)

The Landrazza valley is part of the Manie Plateau, located on the southern side of the Ligurian Alps. It is located at a height of about 270 m, north of the town of Noli (Sv). The section of the valley involved with prospecting is a karst depression that is part of the Landrazza Cockpit (Biancotti *et al.*, 1991). It is a large valley with a flat bottom oriented along a NE-SW direction and converges, with a slight longitudinal slope, into the main valley of the cockpit, oriented in the E-W direction. Both valleys, lying along fragile tectonic lines, are covered by colluvial deposits of «terre rosse». The steep slopes which encircle the bottom of the valley consist lithologically of meso-triassic dolomite rock of the Dolomite formation of S. Pietro ai Monti and by talus of the same formation. The «terre rosse» is generally not very permeable since it consists of more or less sandy-slimy residual clay with a variable large fraction. The dolomite rock and the talus have greater permeability, respectively due to karst phenomena and/or fracturing and porosity.

The general scheme of the surveyed area, with the structural assessment and geophysical surveys, is shown in fig. 7. Profiles AA′ and BB′, which are orthogonal to the valley axis, were performed with configurations 1 and 2 of fig. 2, using square sides of 1 and 2 m. The same profiles were also surveyed with classical tripotential devices and always with spacing of 1 and 2 m. The lower part of the valley was also subjected to an areal coverage (CDEF) with configuration 3 of fig. 2 and finally a set of square soundings with configurations 4 and 5, always of fig. 2, were performed. The latter measurements were compared with the classical Wenner and Schlumberger VES developed in the same square sounding directions.

The development of the values in profiles AA′ and BB′ are very similar due to the regularity of the valley section, and therefore we will limit our discussion of the results only to the second profile. Figure 8 reports the values relative to the square measurements with configuration 1 and sides 1 and 2 m. The resistivities $\rho_\alpha$ and $\rho_\beta$, for $a$ = 1 m, show maximums centered at 22 and 42 m with a more regular development for $\rho_\alpha$. $R_\gamma$ has a rather marked oscillatory development around lower values.

The values relative to $a$ = 2 m show a different development since, due to the larger dimensions of the array, the survey depth is greater and thus also involves the calcareous bedrock. There is a sharp variation at the 20 m position. The resistivities $\rho_\alpha$ and $\rho_\beta$ are lower than those obtained with spacing $a$ = 1 m in the initial part of the profile, while the situation is reversed in the final part of the profile (towards E) with a clear involvement of the deep levels belonging to the dolomitic limestones of the bedrock. There are no substantial differences in $R_\gamma$ in the two dimensions of the array except perhaps for a greater oscillation frequency for $a$ = 1 m. The values corresponding to the average resistivity $\rho_m$ offer a more regular behaviour of the irregularities observed for both $\rho_\alpha$ and $\rho_\beta$.

The same profile BB′ was evaluated with configuration 2 (fig. 2). The developments in the various configurations are reported in fig. 9. It can be seen by comparing the resistivities $\rho_\alpha$ and $\rho_\beta$ with the corresponding ones for the array 1 (fig. 8) that there are no significant differences between the values relative to 1 m spacing, while some small variations are evident for $a$ = 2 m.

Considering that for the $\alpha$ configuration in array 1 the energization electrodes are directed along the valley axis while for $\beta$ measurements they are in a perpendicular direction, and considering also that for configuration 2 the current electrodes for the $\alpha$ and $\beta$ measurements are positioned at 45° from the direction of the

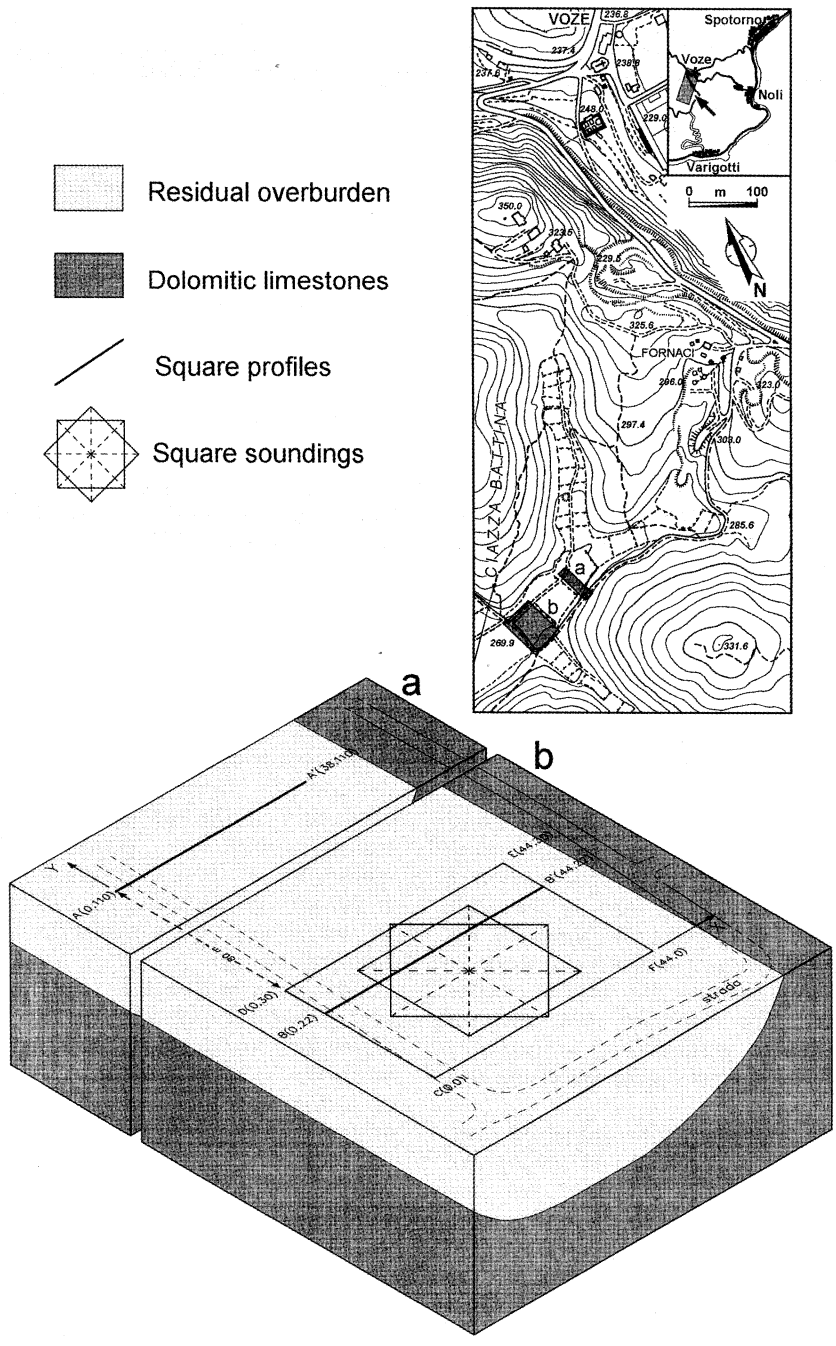


**Fig. 7.** Landrazza valley. Map of the investigated areas and scheme of the square measurements performed (profiles, maps and soundings).

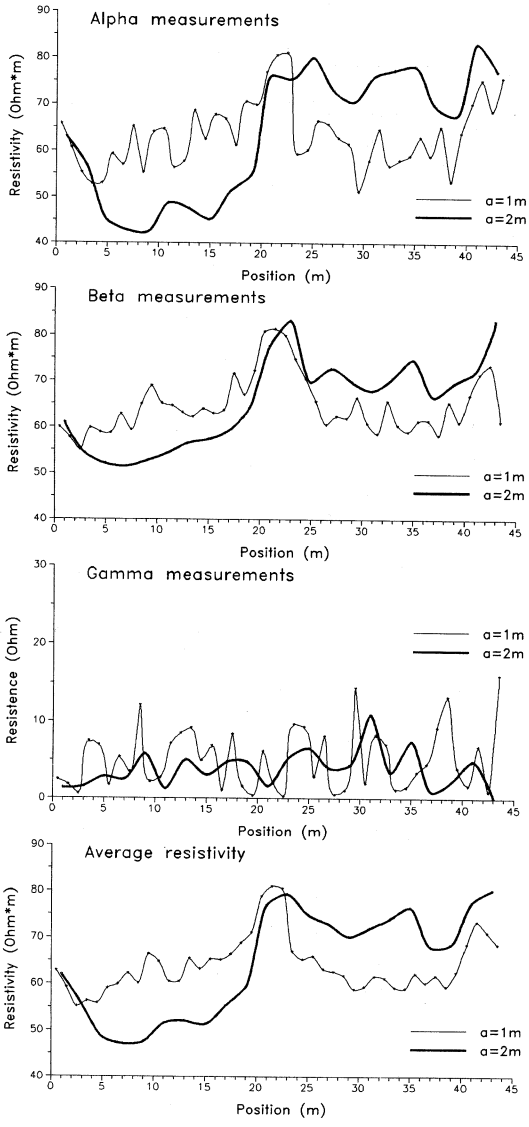


**Fig. 8.** Landrazza valley: square values in profile BB′ obtained with array 1 of fig. 2.

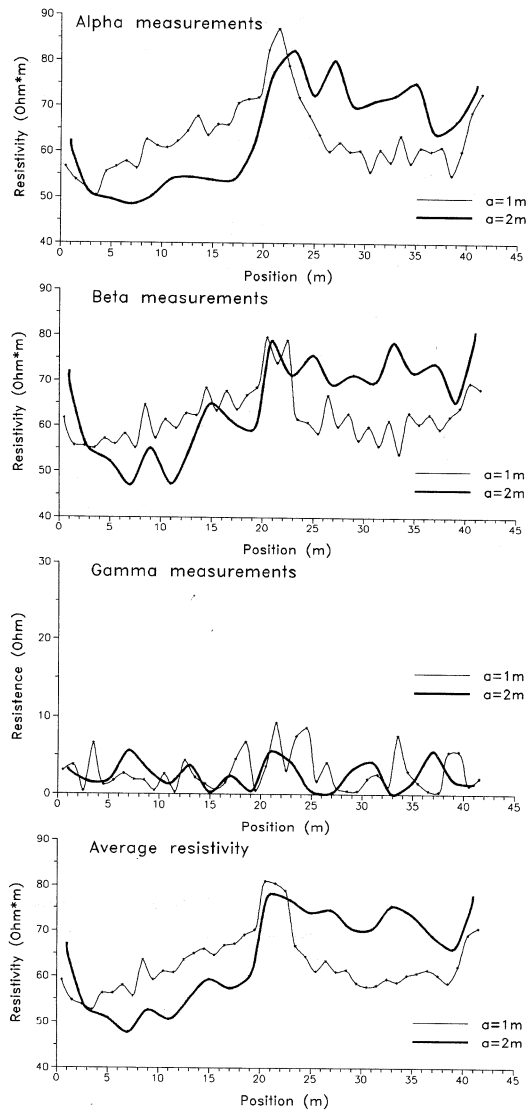


**Fig. 9.** Landrazza valley: square values in profile BB′ obtained with array 2 of fig. 2.

valley axis, it follows that the difference in the values of the two resistivities for array 1 implies a maximum in the conductivity in the direction of the valley axis and a minimum in the perpendicular direction. Instead, this difference is not measured when electrodes are located at 45° from both directions (array 2). However, by comparing the average resistivities in the two configurations, it was found that there is no difference for the results obtained with the two arrays either for $a = 1$ m and $a = 2$ m. This confirms that for the case examined the direc-

tional differences are cancelled by the averaging operation.

It is interesting to examine the values obtained with a linear tripotential array on the BB′ profile. They are reported in fig. 10 for 1 and 2 m spacing. It can be seen that the developments are very similar to those obtained with the square array, at least for the values $\rho_\alpha$ and $\rho_\beta$ but with a more marked oscillatory behavior.

The areal survey of the CDEF sector was performed using array 3 shown in fig. 2 and setting $a = 2$ m. There $\rho_\alpha$ corresponds to measurements with current electrodes in the direction of the valley axis and $\rho_\beta$ in the orthogonal direction. The general development shown in the map relative to $\rho_\alpha$ (fig. 11a) is very similar to what was already indicated only by profile BB′, *i.e.* the presence of areas with resistivities on two different levels, separated by a transition zone, in which the gradient is a maximum, between 18 and 22 m, in a transverse direction to the valley. Instead, the map relative to $\rho_\beta$ (fig. 11b) shows elements which are mainly extended in the direction of the valley axis.

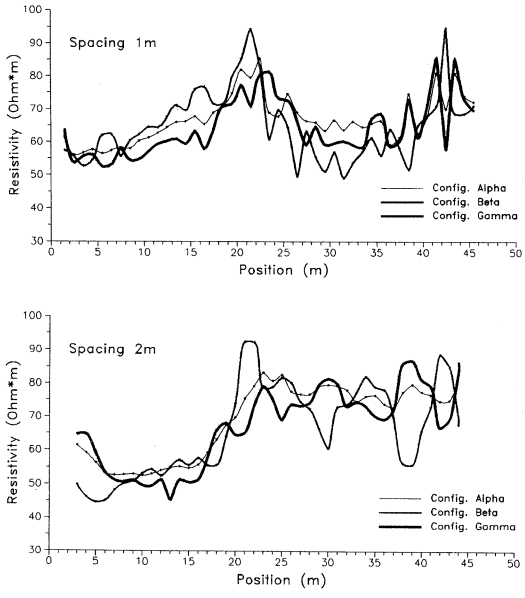


**Fig. 10.** Landrazza valley. Distribution of tripotential resistivity values in profile BB′.

Through a sort of filtering process, $\rho_m$ provides a less «disturbed» representation of the long wavelength anomalies, highlighting the much more interesting variations of the calcareous bedrock. The three-dimensional representation of the development of $\rho_m$ is reported in fig. 11c. This representation, even if mainly qualitative, effectively enhanced the previous observations.

Different types of vertical electric soundings were performed in this same area of the valley and with a common station center (15,22). Obviously, the scope was to test the square array also in a sounding configuration and to compare the results with those relative to the most classical Wenner and Schlumberger VES developed along appropriate directions. With the square array, we obtained two simultaneous sounding curves: one with energization according to the $\alpha$ configuration and the other with energization according to the $\beta$ configuration. The two experimental curves only coincide for a homogeneous subsoil.

The square soundings were performed by expanding the array by $\sqrt{2}$ from the initial dimension $a = \sqrt{2}$ m up to the dimension $a = 16\ \sqrt{2}$ m, in accordance with the available space. This expansion factor makes it possible to represent the square data using resistivity curves which are equivalent to the Wenner array and to interpret them in a similar fashion.

One example of electrical stratigraphy obtained with array 4 of fig. 2 is reported in fig. 12. In this configuration the current electrodes for measurement $\beta$ are located in the direction 153°N and those for measurement $\alpha$ in the direction 63°N. In both stratigraphies there is a surface layer, with a thickness of about 1 m, followed by a more resistant level with a slightly greater thickness. This second layer is thicker in the stratigraphy relative to $\rho_\alpha$ compared to that of $\rho_\beta$. The third layer corresponds to the level of the aquifer that has a lower resistivity and thickness of about 2 m. The transition to the substrate occurs through an alteration level that has a rather high resistivity value. The thickness of this level is much greater in the electrical stratigraphy for $\rho_\alpha$ than for $\rho_\beta$.

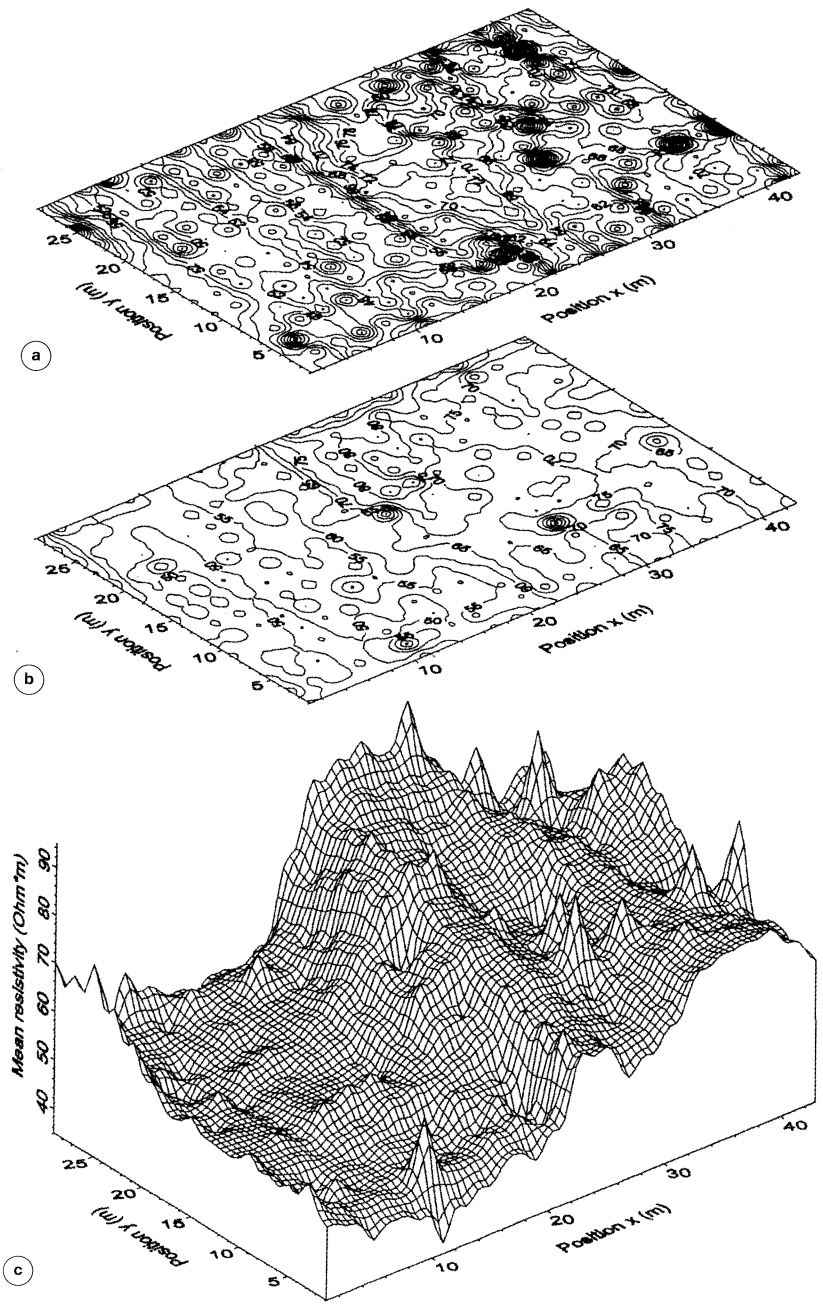


**Fig. 11a-c.** Landrazza valley. Areal coverage of the CDEF sector with array 3 of fig. 2. a) Map of resistivity $\rho_\alpha$; b) map of resistivity $\rho_\beta$; c) three dimensional representation of the distribution of average resistivity $\rho_m$.

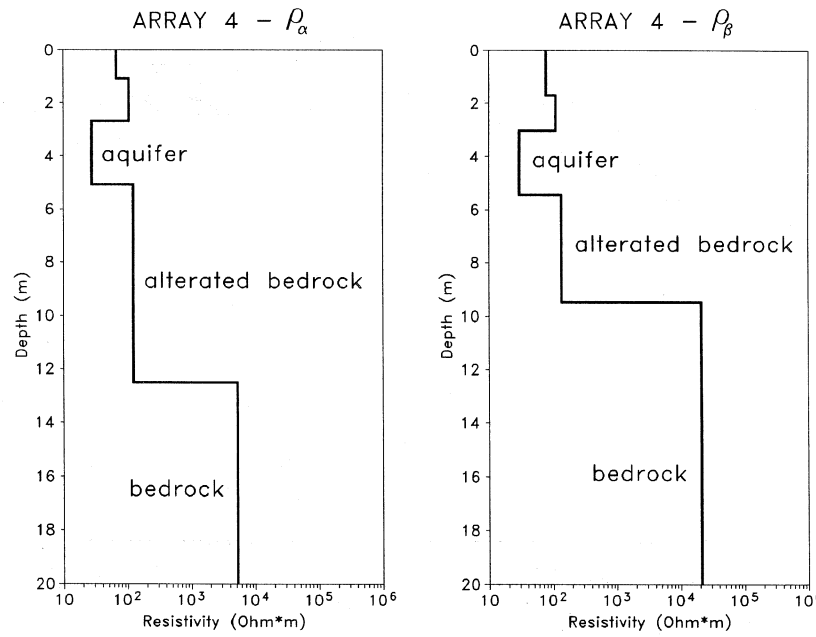


**Fig. 12.** Landrazza valley. Electrical stratigraphies derived from soundings with a square array. Station center (15,22) and array 4 of fig. 2.

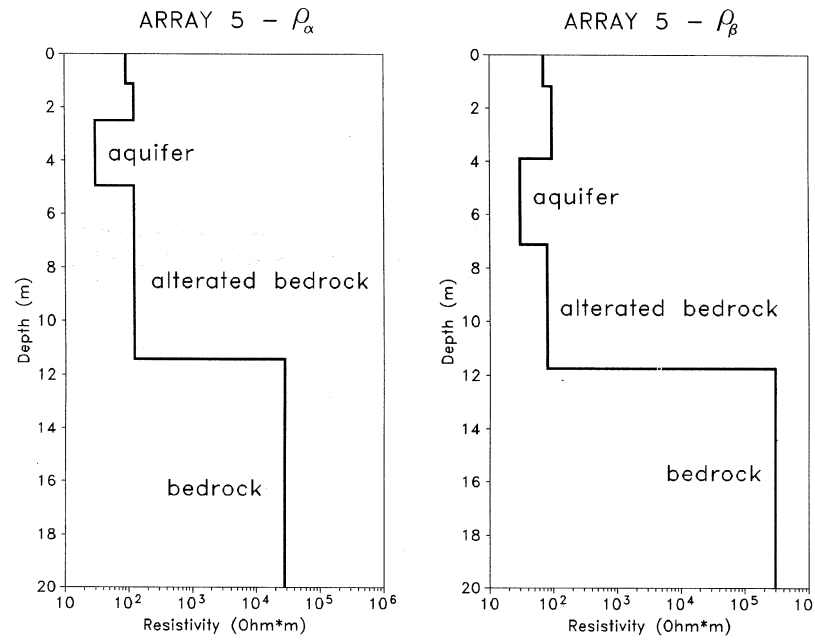


**Fig. 13.** Landrazza valley. Electrical stratigraphies derived from soundings with a crossed square array. Station center (15,22) and array 5 of fig. 2.

The same sounding repeated with array 5 of fig. 2 generated the electrical stratigraphies reported in fig. 13. The second layer is much thicker in stratigraphy $\rho_\beta$ than in $\rho_\alpha$. With this array the resistivity $\rho_\beta$ is obtained with current electrodes placed in the direction 108°N. In this direction the thickness corresponding to the aquifer is greater and the same water table is at a greater depth compared to the other directions. This development confirms what was already measured with the profiles, *i.e.* the increase in resistivity in the rising direction of the calcareous bedrock.

The Wenner and Schlumberger VES were developed according to the direction of the diagonals of the square array and consequently comparisons must be made between homologous elements. To do this, we must refer to the directions of the current electrodes. Therefore, we can consider the resistivity $\beta$ for square device 4 corresponding to the Wenner and Schlumberger VES with directions 153°N; the resistivity $\alpha$ corresponding to the sounding with direction 63°N, while for square array 5 the resistivities $\alpha$ and $\beta$ correspond respectively to soundings 18°N and 108°N. Figure 14 reports the experimental curves obtained with the three arrays. Comparisons may be performed considering the four main directions indicated. It can be seen that the curves of the Wenner and Schlumberger VES, for the directions considered, almost coincide for the initial part while they differ in the final part where the Wenner is more sensitive to the lateral variations.

The square sounding curves $\rho_\alpha$ and $\rho_\beta$ for array 4 (fig. 2) have the same development but on different resistivity values. In particular, the $\rho_\alpha$ curve is always less than the corresponding $\rho_\beta$. Recalling that the $\alpha$ measurement is performed with the current electrodes positioned in the direction of the valley axis, we can state that the conductivity in this direction is greater than that in the transverse direction. This difference, which was not immediately observable in the profiles, is instead quite evident in the square sounding curves, probably due to the greater survey depth and therefore to the greater influence of the bedrock.

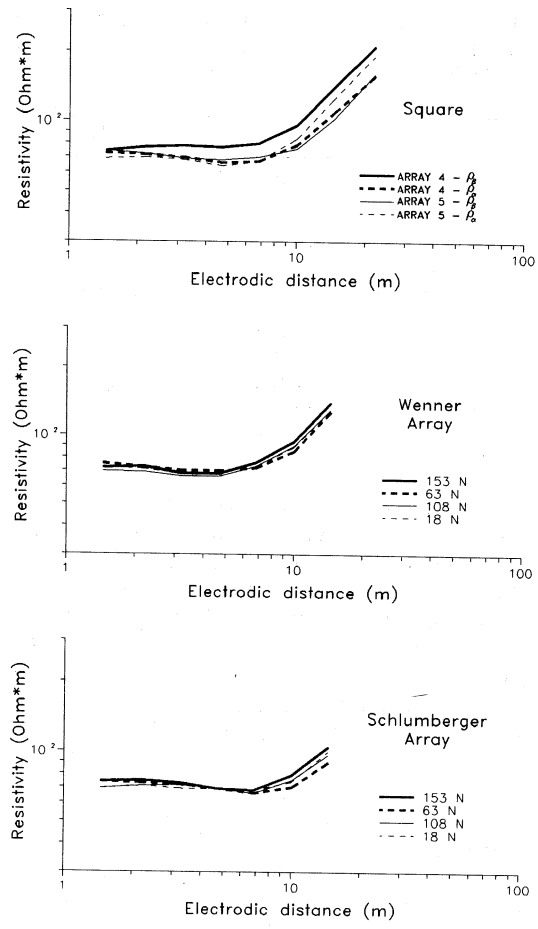


**Fig. 14.** Landrazza valley. Comparison between the experimental curves of the VES performed with square, Wenner and Schlumberger arrays, according to the four equivalent directions.

With configuration 5 (fig. 2), the developments of $\rho_\alpha$ and $\rho_\beta$ are different from the previous ones. In particular, $\rho_\alpha$ seems to feel the effects of the bedrock prior to $\rho_\beta$. This fact indicates that the direction along which the coverage/bedrock discontinuity arise is approximately coincident with the direction of the current electrodes ($\alpha$ or $\beta$) in array 5. Naturally, it is difficult to choose between these two directions based only on this information. To find a

**Table I.** Landrazza valley. Values of the AIR ($\alpha-\beta$) coefficients calculated for the square VES performed with arrays 4 and 5 of fig. 2.

| Array 4 | | | Array 5 | | |
|---|---|---|---|---|---|
| $a$ | AIR($\alpha-\beta$) | AIR($\gamma$) | $a$ | AIR($\alpha-\beta$) | AIR($\gamma$) |
| $\sqrt{2}$ | −0.03 | 0.02 | $\sqrt{2}$ | −0.08 | 0.06 |
| $2\sqrt{2}$ | −0.09 | 0.04 | $2\sqrt{2}$ | −0.01 | 0.09 |
| $4\sqrt{2}$ | −0.17 | 0.2 | $4\sqrt{2}$ | −0.18 | 0.07 |
| $8\sqrt{2}$ | −0.27 | 0.06 | $8\sqrt{2}$ | 0.26 | 0.02 |
| $16\sqrt{2}$ | −0.45 | 0.07 | $16\sqrt{2}$ | 0.18 | 0.33 |

solution it would be necessary to rotate the array over a smaller angular interval. In our case, since the results of the profiles are also available, it is plausible to state that the bedrock rises in a direction near to 108°N.

The values of the coefficients AIR($\alpha-\beta$) and AIR($\gamma$) calculated starting from square soundings according to configurations 4 and 5, are reported in table I. AIR($\alpha-\beta$) for array 4 is always negative and therefore $\rho_\beta$ is always greater than $\rho_\alpha$. This fact is clear by simply observing the resistivity curves (fig. 14) and therefore, at least in our case, AIR($\alpha-\beta$) does not add new information. In addition, it can be seen that the coefficients have higher values for greater spacing. This can be related to the anisotropy effect introduced by a greater involvement of the bedrock. However, overall, the results of table I have little importance while the direct comparison between the resistivity curves provides greater and more detailed information.

## 5. Conclusions

The results from the experimental applications of the square array technique were used to confirm some of the theoretical properties attributed to this electrical array.

From an operating point of view, the square acquisition procedure was more demanding, with respect to the classical linear devices, in performing profiles and, to a lesser degree, in performing vertical electric soundings.

In fact, for profiles, the significance of the measurements obtained is comparable to what can be obtained with the linear tripotential technique but, with respect to the latter, the square array involves a greater amount of work, requiring a double line of electrodes to perform a single profile. The evaluation is more favourable for soundings, since a square sounding is equivalent, in terms of amount of information, to two crossed linear soundings. Furthermore, the square technique is much faster than the linear ones since it is possible, for each spacing of the electric sounding, to manage the three measurements $\alpha$, $\beta$ and $\gamma$ directly from the control device, using a function switch.

Considering the experiments in the Marzabotto area, it was found that even though the square array provided some additional information relative to the directional anisotropy of the surveyed structures, it basically did not modify the conclusions derived only from linear tripotential prospecting. Therefore, we can state that when performing profiles, the square array provides reliable results, but only slightly more information compared to the tripotential technique.

Substantially different remarks can be made for vertical electric soundings. From the limited applications of the sounding configuration performed in the Landrazza Valley it was

found that the square array can be used to obtain greater and more significant information compared to the classical vertical electric sounding arrays. In fact, while the response of all the arrays is similar in what are mainly uniform areas, the response is clearly improved by the square measurements in areas involving directional anisotropy.

Major doubts have arisen from the analysis of the experimental data on the meaning and the use of the anisotropy coefficients $\mathrm{AIR}(\alpha-\beta)$, $\mathrm{AIR}(\gamma)$ and the error term $v$ as they are defined theoretically. These parameters were found to have limited use for characterizing the anisotropy of the ground and for verifying the reliability of the measurements. The same information is obtained, without a great loss in meaning, directly from the resistivity values.

In conclusion, we can state that the square array technique is certainly useful and more exhaustive than the classical linear arrays in performing soundings since its provides information on the distribution of the anisotropy in the subsoil. Instead, considering the survey work required, there are less application advantages in performing profiles.

*REFERENCES*


BARKER, R.D. (1981): The offset system of electrical resistivity sounding and its use with a multicore cable, *Geophys. Prospect.*, **29**, 128-143.

BIANCOTTI, A., G. BRANCUCCI and M. MOTTA (1991): Note illustrative della carta geomorfologica dell'Altopiano delle Manie e dei bacini idrografici limitrofi (Liguria Occidentale), *Studi e Ricerche di Geografia*, **14** (2), 12-25.

BOZZO, E., S. LOMBARDO, F. MERLANTI and M. PAVAN (1994): Integrated geophysical investigations at an Etrurian Settlement in Northern Appennines (Italy), *Archaeological Prospection*, **1** (1), 19-36.

CARPENTER, E.W. (1955): Some notes concerning the Wenner configuration, *Geophys. Prospect.*, **3**, 388-402.

CARPENTER, E.W. and G.M. HABBERJAM (1956): A tripotential method of resistivity prospecting, *Geophysics*, **21**, 455-469.

HABBERJAM, G.M. (1972): The effects of anisotropy in square array resistivity measurements, *Geophys. Prospect.*, **20**, 249-266.

HABBERJAM, G.M. (1979): *Apparent Resistivity Observation and the Use of Square Array Techniques*, Geoexploration Monographs, Series 1, No. **9** (Gebruder Borntraeger, Berlin), pp. 149.

MERLANTI, F. (1990): Misure geoelettriche in corrente continua con dispositivo multielettrodico, in *Atti IX Convegno GNGTS*, Roma 1990, 489-499.

SASSATELLI, G. (1989): *La Città Etrusca di Marzabotto* (Grafis Ed., Bologna), pp. 92.

SASSATELLI, G. and A.M. BRIZZOLARA (1990): *I Nuovi Scavi dell'Università di Bologna nella Città Etrusca di Marzabotto* (CLUEB Ed., Bologna), pp. 47.